Modal Analysis of a Planar Waveguide with Gain and Losses

T. D. Visser, H. Blok, *Member, IEEE*, and D. Lenstra

***Abstract*—In this study, we analyze the waveguiding properties of a planar waveguide amplifier in which losses and gain can be present simultaneously. It is found that the subsequent modes comprise both loss and gain modes. Also, the dependence of the gain on the state of polarization turns out to be significant for realistic dielectric structures. For strong losses or gain, the standard transfer matrix approach may become numerically unstable, therefore, a scattering matrices formalism is employed. A semiconductor-like gain profile enables us to study the gain as a function of ω for realistic laser amplifier structures.**

I. Introduction

FOR optical telecommunication it is highly desirable that the amplification of attenuated light signals is independent of the state of polarization. The reason is that the polarization is not maintained during propagation in optical fibers.

The motivation of this study is a reported semiconductor optical amplifier which, indeed, does not show the typical difference in gain for TE and TM input signals [1]. This device has multiple quantum wells with tensile and compressive strain.

In this paper, the waveguiding properties of a planar configuration in which both active and lossy media can be present are analyzed. The formalism is fully vectorial and completely rigorous. The use of the numerically stable scattering matrices method allows us to analyze structures in which the gain and losses are very strong. This in contrast to the usual transfer matrix approach which may fail in such situations. The dependence of the gain per unit of length on the thickness of the active layer, its refractive index, the frequency, and the state of polarization is examined. Attention is paid to the numerical aspects of modeling high gain and losses. For a review of waveguide modeling techniques see [2], [3].

Generally, it is believed that due to the difference in confinement to the active layer, the gain for TE fields will differ from that for TM fields [4], [5]. We will argue that that view is not entirely correct. One result of our study is the analysis of a realistic example in which the gain for the two polarization states differs substantially, even though the confinement factors are comparable. As is now derived, the expression connecting gain and confinement for TE modes differs from that for TM modes [6].

Manuscript received February 1, 1995; revised June 19, 1995. This work is supported in part by the Technology Foundation (STW). The work contributed by H. Blok was supported by a grant from the Schlumberger Fund for Science, Technology and Research.

T. D. Visser is with the Department of Physics and Astronomy, Free University, De Boelelaan 1081, 1081 HV Amsterdam, The Netherlands and the Laboratory of Electromagnetic Research, Department of Electrical Engineering, Delft University of Technology, P.O. Box 5031, 2600 GA Delft, The Netherlands.

H. Blok is with the Laboratory of Electromagnetic Research, Department of Electrical Engineering, Delft University of Technology, P.O. Box 5031, 2600 GA Delft, The Netherlands.

D. Lenstra is with the Department of Physics and Astronomy, Free University, De Boelelaan 1081, 1081 HV Amsterdam, The Netherlands.

IEEE Log Number 9414178.

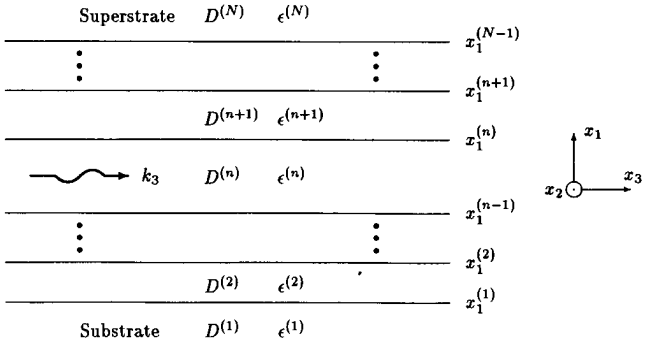

Fig. 1. Geometry of a planar waveguiding structure. N-2 layers are sandwiched between a superstrate and a substrate that are both semi-infinite. The wave propagates in the positive x_3-direction with complex propagation constant k_3. Each permittivity $\epsilon^{(i)}$ may have either a positive or a negative imaginary part. The coordinate $x_1^{(n)}$ indicates the position of the interface between the layers $D^{(n)}$ and $D^{(n+1)}$.

II. Formulation of the Problem

As a first model for a semiconductor laser amplifier that allows one to investigate the dependence of the gain on the state of polarization, we take a waveguide that is stratified in the vertical or x_1-direction (see Fig. 1). It is made up of homogeneous layers of isotropic dielectric material, which extend from minus to plus infinity in the x_2- and x_3-directions. In the steady state [time-harmonic light signals are assumed with complex time dependence $\exp(j\omega t)$], the imaginary part of the complex permittivity ϵ can be either positive (corresponding with active media) or negative (corresponding with lossy media). Gain and losses may be present simultaneously in different layers. It is also possible to use a negative conductivity to simulate gain. This has been done, e.g., by Hawkins and Kallman [7].

Starting point is the Maxwell equations for the steady state in a source-free region

$$-\nabla \times \hat{\mathbf{H}} + j\omega\epsilon\hat{\mathbf{E}} = 0 \tag{1}$$

$$\nabla \times \hat{\mathbf{E}} + j\omega\mu_0\hat{\mathbf{H}} = 0. \tag{2}$$

The arguments of the fields $\hat{\mathbf{H}}$ and $\hat{\mathbf{E}}$ are $\{x_1, x_2, x_3, j\omega\}$. The layers are assumed to be homogeneous, isotropic, nonmagnetic, nonconducting, and linear. The relevant boundary

conditions are that $\hat{E}_2, \hat{E}_3, \hat{H}_2$ and $\hat{H}_3$ are continuous across the interfaces between the layers. The polarization $\mathbf{P}$ in the space-time domain for materials with time relaxation is given by

$$\mathbf{P}(\mathbf{x},t) = \int_0^\infty \epsilon_0 \chi(\mathbf{x},t')\mathbf{E}(\mathbf{x},t-t')\,dt' \tag{3}$$

where χ denotes the susceptibility. For the time-harmonic fields that we study, this gives for the constitutive relation in the frequency domain

$$\hat{\mathbf{D}}(\mathbf{x},j\omega) = \epsilon_0(1+\hat{\chi}(\mathbf{x},j\omega))\hat{\mathbf{E}}(\mathbf{x},j\omega) = \epsilon(\mathbf{x},j\omega)\hat{\mathbf{E}}(\mathbf{x},j\omega). \tag{4}$$

We choose a multiple Lorentzian line shape for the frequency dependence of the permittivity ϵ. The expression for ϵ due to Z stimulated emission and/or absorption lines is given by [8, ch. 3]

$$\epsilon(\omega) = \epsilon_r\epsilon_0\left[1+\sum_{i=1}^{Z}\frac{2I_i}{\omega^2-\omega_i^2-j\omega\gamma_i}\right]. \tag{5}$$

Here ω_i is the i^{th} resonance frequency, γ_i its line width and I_i its normed intensity. In our examples, we characterize the different media by their (bulk) refractive index $n = c(\epsilon\mu)^{1/2}$. If $\mathrm{Im}\{n\} > 0$, we have a gain medium, if $\mathrm{Im}\{n\} < 0$, the medium is lossy.

To analyze the propagation properties, we are looking for solutions that represent guided modes that propagate in the positive x_3-direction, i.e., solutions for the fields which are of the form

$$\{\hat{\mathbf{E}},\hat{\mathbf{H}}\}(x_1,x_3;K) = \{\tilde{\mathbf{E}},\tilde{\mathbf{H}}\}(x_1;K)\exp[-jk_3x_3]. \tag{6}$$

Here $K = k_3/k_0$ is the mode or effective index, with k_3 the (complex) propagation constant of the mode, and $k_0 = \omega/c$ the free-space wavenumber. The phase velocity in the longitudinal x_3-direction equals $\omega[k_0\mathrm{Re}\{K\}]^{-1}$. If $\mathrm{Im}\{K\} > 0$, then the field amplitude increases during propagation. We then speak of gain modes. In the case of loss modes, $\mathrm{Im}\{K\} < 0$ and the field amplitude decreases during propagation.

We restrict ourselves to the case where the index of refraction does not change along x_3, i.e., we do not treat nonlinear effects. In many realistic systems, such effects are present and should be taken into account. We are presently pursuing this using an integral equation method. This publication is an essential ingredient for that project.

We will often consider the modal power gain of a waveguide. It can be expressed either as the gain coefficient g

$$g = 2\,\mathrm{Im}\{k_3\} = 2k_0\,\mathrm{Im}\{n_{\text{eff}}\}\,[\mathrm{m}^{-1}] \tag{7}$$

or as the gain in dB per unit length, e.g.,

$$\text{gain} = 10\times{}^{10}\log\left(e^{2\,\mathrm{Im}\{k_3\}10^{-4}}\right)\,[\text{dB/100 }\mu\text{m}]. \tag{8}$$

III. TE and TM Modes

The configuration is invariant in the x_2- and x_3-directions. The wave propagates in the x_3-direction and the fields are assumed to be independent of x_2, hence, $\partial_2 = 0$. As is well known, the Maxwell equations now separate into two independent sets of three relations [9]. One set describes transverse magnetic (TM) fields with $\{\hat{\mathbf{H}}_2,\hat{\mathbf{E}}_1,\hat{\mathbf{E}}_3\} \neq 0$. The other one describes transverse electric (TE) fields with $\{\hat{\mathbf{E}}_2,\hat{\mathbf{H}}_1,\hat{\mathbf{H}}_3\} \neq 0$.

TM Modes: For the guided modes of the TM type, we find through direct substitution of (6) the equations

$$-jk_3\tilde{H}_2 + j\omega\epsilon\tilde{E}_1 = 0, \tag{9}$$

$$-\partial_1\tilde{H}_2 + j\omega\epsilon\tilde{E}_3 = 0, \tag{10}$$

$$-jk_3\tilde{E}_1 - \partial_1\tilde{E}_3 + j\omega\mu_0\tilde{H}_2 = 0. \tag{11}$$

In these equations only $\tilde{E}_1, \tilde{E}_3$ and $\tilde{H}_2$ occur. In the TM modes the magnetic field is perpendicular to the direction of propagation x_3. It is solely directed along x_2, parallel to the interfaces. The electric field has one component along x_3 and another one in the stacking or x_1-direction.

TE Modes: In an identical manner, we find for the TE guided modes that

$$\partial_1\tilde{H}_3 + jk_3\tilde{H}_1 + j\omega\epsilon\tilde{E}_2 = 0, \tag{12}$$

$$jk_3\tilde{E}_2 + j\omega\mu_0\tilde{H}_1 = 0, \tag{13}$$

$$\partial_1\tilde{E}_2 + j\omega\mu_0\tilde{H}_3 = 0. \tag{14}$$

In these relations, only $\tilde{E}_2, \tilde{H}_1$ and $\tilde{H}_3$ play a role. In the TE modes the electric field is perpendicular to the direction of propagation x_3. It is solely directed along x_2, parallel to the interfaces. The magnetic field has a component along x_3 and one in the stacking or x_1-direction. In general, the total field will be a superposition of TE and TM fields.

IV. The System Matrix

Each set of equations, (9)–(11) or (12)–(14), consists of one algebraic, (9) or (13), and two differential equations. These algebraic equations can be used to eliminate the field components that are discontinuous at the interfaces. In this way, we find in each layer $D^{(n)}$ the field matrix equation

$$\partial_1\mathbf{f} = \mathbf{A}\mathbf{f} \tag{15}$$

in which for TE fields the field vector is introduced as

$$\mathbf{f} \equiv (\tilde{E}_2, \tilde{H}_3)^T \tag{16}$$

and the system matrix $\mathbf{A}$ is given by

$$\mathbf{A} \equiv j\begin{pmatrix} 0 & -\omega\mu_0 \\ {k_3}^2/(\omega\mu_0) - \omega\epsilon^{(n)} & 0 \end{pmatrix}. \tag{17}$$

Notice that for given angular frequency ω and $\epsilon^{(n)}$, $\mathbf{A}$ depends on the yet to be determined guided-mode propagation constant k_3 only. It will turn out that only for certain discrete values of k_3 solutions of (15) exist. Following [10], we will now proceed to diagonalize (15).

The corresponding field vector equations for the TM fields are found through the substitutions

$$\{\tilde{E}_2, \tilde{H}_3, \epsilon^{(n)}, \mu_0\} \longrightarrow \{\tilde{H}_2, \tilde{E}_3, -\mu_0, -\epsilon^{(n)}\}. \quad (18)$$

We only treat the TE modes explicitly. In Section VII, results for both states of polarization will be presented.

A. Analysis of the System Matrix

Notice that the matrix $\mathbf{A}$ is singular if (and only if)

$$\omega^2 \epsilon^{(n)} \mu_0 = {k_3}^2. \quad (19)$$

Since fields satisfying (19) can only occur in free space, we may safely assume that the system matrix is nonsingular for the guided-mode solutions. The system matrix $\mathbf{A}$ is of the form

$$\mathbf{A} \equiv \begin{pmatrix} 0 & a_{12}^{(n)} \\ a_{21}^{(n)} & 0 \end{pmatrix} \quad (20)$$

and has eigenvalues $\lambda_2^{(n)} = -\lambda_1^{(n)} = -(a_{21}^{(n)} a_{12}^{(n)})^{1/2}$. The square root is chosen such that $\mathrm{Im}\{\lambda_1^{(n)}\} < 0$. A convenient choice for the eigenvectors will turn out to be

$$\mathbf{v}_1^{(n)} = \begin{pmatrix} (a_{12}^{(n)})^{1/2} \\ (a_{21}^{(n)})^{1/2} \end{pmatrix}$$

and

$$\mathbf{v}_2^{(n)} = \begin{pmatrix} -(a_{12}^{(n)})^{1/2} \\ (a_{21}^{(n)})^{1/2} \end{pmatrix} \quad (21)$$

where the subscripts 1 and 2 refer to the eigenvalues $\lambda_1^{(n)}$ and $\lambda_2^{(n)}$, respectively. Since $\mathbf{A}$ is nonsingular, $a_{21}^{(n)} a_{12}^{(n)} \neq 0$, and hence, the two eigenvalues are nondegenerate.

$\mathbf{A}$ can be diagonalized by a similarity transformation:

$$(\mathbf{C}^{(n)})^{-1} \mathbf{A} \mathbf{C}^{(n)} = \mathbf{\Lambda}^{(n)}. \quad (22)$$

Here, the composition matrix $\mathbf{C}^{(n)}$ is given by

$$\mathbf{C}^{(n)} \equiv \begin{pmatrix} \mathbf{v}_1^{(n)} & \mathbf{v}_2^{(n)} \end{pmatrix} = \begin{pmatrix} (a_{12}^{(n)})^{1/2} & -(a_{12}^{(n)})^{1/2} \\ (a_{21}^{(n)})^{1/2} & (a_{21}^{(n)})^{1/2} \end{pmatrix} \quad (23)$$

and for the decomposition matrix $(\mathbf{C}^{(n)})^{-1}$ holds

$$(\mathbf{C}^{(n)})^{-1} = \frac{1}{2} \begin{pmatrix} 1/(a_{12}^{(n)})^{1/2} & 1/(a_{21}^{(n)})^{1/2} \\ -1/(a_{12}^{(n)})^{1/2} & 1/(a_{21}^{(n)})^{1/2} \end{pmatrix}. \quad (24)$$

Notice that in this particular case, the nonsingularity of $\mathbf{A}$ implies the nonsingularity of $\mathbf{C}$. The diagonal matrix $\mathbf{\Lambda}^{(n)}$ equals

$$\mathbf{\Lambda}^{(n)} \equiv \begin{pmatrix} \lambda_1^{(n)} & 0 \\ 0 & \lambda_2^{(n)} \end{pmatrix}. \quad (25)$$

Using $\mathbf{A} = \mathbf{C}^{(n)} \mathbf{\Lambda}^{(n)} (\mathbf{C}^{(n)})^{-1}$, and defining the wave function vector $\mathbf{w}^{(n)}$ as

$$\mathbf{w}^{(n)} \equiv (\mathbf{C}^{(n)})^{-1} \mathbf{f}^{(n)} \quad (26)$$

we find that the differential equation (15) can be formulated in terms of this wave function vector in a diagonalized form as

$$\partial_1 \mathbf{w}^{(n)} = \mathbf{\Lambda}^{(n)} \mathbf{w}^{(n)}. \quad (27)$$

The solutions are simply

$$\mathbf{w}^{(n)}(x_1) = \exp\left(\mathbf{\Lambda}^{(n)}[x_1 - x_1^{\mathrm{ref}}]\right) \mathbf{w}^{(n)}(x_1^{\mathrm{ref}}) \quad (28)$$

with $x_1, x_1^{\mathrm{ref}} \in D^{(n)}$ and $\mathbf{w}^{(n)}(x_1^{\mathrm{ref}})$ the wave function vector at a certain reference level $x_1 = x_1^{\mathrm{ref}}$ in layer $D^{(n)}$, i.e.,

$$\mathbf{w}^{(n)}(x_1^{\mathrm{ref}}) = (\mathbf{C}^{(n)})^{-1} \mathbf{f}^{(n)}(x_1^{\mathrm{ref}}). \quad (29)$$

Since Λ is diagonal, this can be rewritten as

$$\begin{pmatrix} w_+^{(n)}(x_1) \\ w_-^{(n)}(x_1) \end{pmatrix} = \begin{pmatrix} \exp[\lambda_1^{(n)}(x_1 - x_1^{\mathrm{ref}})] & 0 \\ 0 & \exp[-\lambda_1^{(n)}(x_1 - x_1^{\mathrm{ref}})] \end{pmatrix} \times \begin{pmatrix} w_+^{(n)}(x_1^{\mathrm{ref}}) \\ w_-^{(n)}(x_1^{\mathrm{ref}}) \end{pmatrix}. \quad (30)$$

Since we had chosen $\mathrm{Im}\{\lambda_1^{(n)}\} < 0$, this means (together with the time-dependence $\exp[j\omega t]$) that $w_+^{(n)}(x_1)$ represents a wave traveling in the positive x_1-direction, whereas $w_-^{(n)}(x_1)$ represents a wave that travels in the negative x_1-direction. Both waves have a transversal wavenumber $k_1^{(n)} = j\lambda_1^{(n)}$. Since $\lambda_i^{(n)} = \lambda_i^{(n)}(k_3)$ it follows that $k_1^{(n)}$ also depends on the yet to be determined longitudinal wavenumber k_3.

Using that $\mathbf{w} = (\mathbf{C})^{-1}\mathbf{f}$, the solution of our original expression (15) for the TE fields is

$$\mathbf{f}(x_1) = \mathbf{T}(x_1, x_1')\mathbf{f}(x_1'), \quad x_1, x_1' \in D^{(n)} \quad (31)$$

with

$$\mathbf{T}^{(n)}(x_1, x_1') \equiv \mathbf{C}^{(n)} \exp\left(\mathbf{\Lambda}^{(n)}[x_1 - x_1']\right)(\mathbf{C}^{(n)})^{-1}. \quad (32)$$

Because of the continuity of $\mathbf{f}$ across the interfaces, the field vectors in two points that are located in different layers are connected by a product of such transfer matrices.

In the case of losses and/or gain, the eigenvalue $\lambda_1^{(n)}$ is complex and the elements of the transfer matrix in (30) may differ in orders of magnitude. A product of such matrices will lead to numerical instabilities. Therefore, we resort to a so-called scattering matrices approach because there such difficulties are avoided, even for very strong losses and gain. With these scattering matrices the modal analysis can be carried out. This leads for a given angular frequency ω to the so-called resonance condition, and eventually to the propagation constants $k_3(\omega)$.

V. Scattering Matrices

The transfer matrix connects the wave function vectors $(w_+^{(n)}, w_-^{(n)})$ in two different points. The scattering matrix, however, relates the waves that are incident on a section with the waves that are scattered from that section

$$\begin{pmatrix} w_+^{(n)}(x_1') \\ w_-^{(n)}(x_1) \end{pmatrix} = \mathbf{S}(x_1, x_1') \begin{pmatrix} w_-^{(n)}(x_1') \\ w_+^{(n)}(x_1) \end{pmatrix}. \quad (33)$$

It follows from (30), that the scattering matrix $\mathbf{S}$ is of the form

$$\mathbf{S}(x_1, x_1') = \begin{pmatrix} 0 & \exp[-\lambda_1^{(n)}(x_1 - x_1')] \\ \exp[-\lambda_1^{(n)}(x_1 - x_1')] & 0 \end{pmatrix}. \quad (34)$$

Notice that the signs of the exponentials in S are the same. This will prevent the loss of numbers during actual calculations. The interpretation of the scattering formalism is elucidated in Fig. 2.

A. The Scattering Matrix Between Two Interfaces

Using the continuity of the field vector f across the interfaces, we get from (31) that

$$\lim_{\delta \downarrow 0} \mathbf{f}(x_1^{(n-1)} + \delta) = \mathbf{T}^{(n)} \mathbf{f}(x_1^{(n)} + \delta) \tag{35}$$

where

$$\mathbf{T}^{(n)} = \mathbf{T}^{(n)}(x_1^{(n-1)}, x_1^{(n)}). \tag{36}$$

The transfer matrix $\mathbf{T}^{(n)}$ describes propagation through layer $D^{(n)}$ and the interface above it. Since $\mathbf{w}(x_1) = (\mathbf{C}^{(n)})^{-1}\mathbf{f}(x_1)$ if $x_1 \in D^{(n)}$, it follows for infinitesimally small positive δ that

$$\begin{aligned} \mathbf{w}(x_1^{(n-1)} + \delta) &= (\mathbf{C}^{(n)})^{-1}\mathbf{T}^{(n)}\mathbf{C}^{(n+1)} \\ &\quad \times (\mathbf{C}^{(n+1)})^{-1}\mathbf{f}(x_1^{(n)} + \delta) \qquad (37) \\ &= \exp[\mathbf{\Lambda}^{(n)}(x_1^{(n-1)} - x_1^{(n)})] \\ &\quad \times (\mathbf{C}^{(n)})^{-1}\mathbf{C}^{(n+1)}\mathbf{w}(x_1^{(n)} + \delta) \qquad (38) \end{aligned}$$

where we have used (32). Taking the limit $\delta \downarrow 0$ gives

$$\mathbf{w}(x_1^{(n-1)}) = \mathbf{Q}^{(n)}\mathbf{w}(x_1^{(n)}) \tag{39}$$

with

$$\mathbf{Q}^{(n)} \equiv \exp[\mathbf{\Lambda}^{(n)}(x_1^{(n-1)} - x_1^{(n)})](\mathbf{C}^{(n)})^{-1}\mathbf{C}^{(n+1)}. \tag{40}$$

Writing the elements of $\mathbf{Q}^{(n)}$ as q_{ij} and using (23) and (24) leads to

$$\begin{aligned} q_{11}^{(n)} &= \frac{1}{2}\left[\left(\frac{a_{12}^{(n+1)}}{a_{12}^{(n)}}\right)^{1/2} + \left(\frac{a_{21}^{(n+1)}}{a_{21}^{(n)}}\right)^{1/2}\right] \\ &\quad \times \exp\left(-\lambda_1^{(n)} d^{(n)}\right) \qquad (41) \\ q_{12}^{(n)} &= \frac{1}{2}\left[\left(-\frac{a_{12}^{(n+1)}}{a_{12}^{(n)}}\right)^{1/2} + \left(\frac{a_{21}^{(n+1)}}{a_{21}^{(n)}}\right)^{1/2}\right] \\ &\quad \times \exp\left(-\lambda_1^{(n)} d^{(n)}\right) \qquad (42) \\ q_{21}^{(n)} &= \frac{1}{2}\left[\left(-\frac{a_{12}^{(n+1)}}{a_{12}^{(n)}}\right)^{1/2} + \left(\frac{a_{21}^{(n+1)}}{a_{21}^{(n)}}\right)^{1/2}\right] \\ &\quad \times \exp\left(\lambda_1^{(n)} d^{(n)}\right) \qquad (43) \\ q_{22}^{(n)} &= \frac{1}{2}\left[\left(\frac{a_{12}^{(n+1)}}{a_{12}^{(n)}}\right)^{1/2} + \left(\frac{a_{21}^{(n+1)}}{a_{21}^{(n)}}\right)^{1/2}\right] \\ &\quad \times \exp\left(\lambda_1^{(n)} d^{(n)}\right) \qquad (44) \end{aligned}$$

with the thickness of layer $D^{(n)}$ abbreviated as

$$d^{(n)} = x_1^{(n)} - x_1^{(n-1)}. \tag{45}$$

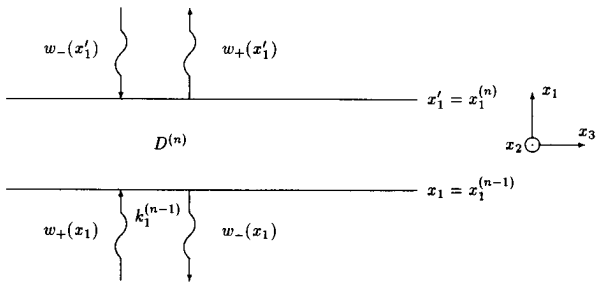

Fig. 2. Interpretation of the scattering matrix. The fields $w_+(x_1)$ and $w_-(x_1')$ are incident on the slab $D^{(n)}$. The fields $w_-(x_1)$and $w_+(x_1')$ are scattered away from this layer. The $w_\pm$ waves propagate in the x_1-direction with (complex) propagation constant k_1. The incident and scattered fields are related by the scattering matrix S.

The above applies for $2 \le n \le N$. For the case $n = 1$ we define

$$\mathbf{Q}^{(1)} \equiv \lim_{\delta \downarrow 0} \mathbf{Q}(x_1^{(1)} - \delta, x_1^{(1)} + \delta) = (\mathbf{C}^{(1)})^{-1}\mathbf{C}^{(2)}. \tag{46}$$

The latter definition will be used later on. The matrix $\mathbf{Q}$ connects the two wave function vectors $(w_+^{(n-1)}, w_-^{(n-1)})$ and $(w_+^{(n)}, w_-^{(n)})$. So for the wave function vectors at two interface levels $x_1^{(n-1)}$ and $x_1^{(m-1)}$ we can write

$$\begin{aligned} \mathbf{w}(x_1^{(n-1)}) &= \mathbf{Q}^{(n)}\mathbf{Q}^{(n+1)} \cdots \mathbf{Q}^{(m-2)}\mathbf{Q}^{(m-1)}\mathbf{w}(x_1^{(m-1)}) \\ &\equiv \mathbf{Q}^{(n,m)}\mathbf{w}(x_1^{(m-1)}). \qquad (47) \end{aligned}$$

Just as before, we want a scattering matrix formalism which relates the incident fields at $x_1^{(n-1)}$ and $x_1^{(m-1)}$ to the scattered fields at the same points. Therefore, define

$$\begin{pmatrix} w_+(x_1^{(m-1)}) \\ w_-(x_1^{(n-1)}) \end{pmatrix} = \mathbf{S}^{(n,m)} \begin{pmatrix} w_-(x_1^{(m-1)}) \\ w_+(x_1^{(n-1)}) \end{pmatrix}. \tag{48}$$

It is readily derived that

$$\begin{aligned} w_+(x_1^{(m-1)}) &= \frac{1}{q_{11}^{(n,m)}} w_+(x_1^{(n-1)}) \\ &\quad - \frac{q_{12}^{(n,m)}}{q_{11}^{(n,m)}} w_-(x_1^{(m-1)}) \qquad (49) \\ w_-(x_1^{(n-1)}) &= \frac{q_{21}^{(n,m)}}{q_{11}^{(n,m)}} w_+(x_1^{(n-1)}) \\ &\quad + \left[q_{22}^{(n,m)} - \frac{q_{21}^{(n,m)} q_{12}^{(n,m)}}{q_{11}^{(n,m)}}\right] w_-(x_1^{(m-1)}). \qquad (50) \end{aligned}$$

This yields the elements of the scattering matrix $\mathbf{S}^{(n,m)}$ as

$$\mathbf{S}^{(n,m)} = \begin{pmatrix} -\frac{q_{12}^{(n,m)}}{q_{11}^{(n,m)}} & \frac{1}{q_{11}^{(n,m)}} \\ q_{22}^{(n,m)} - \frac{q_{21}^{(n,m)} q_{12}^{(n,m)}}{q_{11}^{(n,m)}} & \frac{q_{21}^{(n,m)}}{q_{11}^{(n,m)}} \end{pmatrix}. \tag{51}$$

VI. The Guided Modes

For the N-layer configuration of Fig. 1 we can write down the scattering matrix for two points that lie just within the substrate and superstrate, i.e., we consider the limit $\delta \downarrow 0$ of

$$\begin{pmatrix} w_+(x_1^{(N-1)} + \delta) \\ w_-(x_1^{(1)} - \delta) \end{pmatrix} = \mathbf{S}^{(1,N)} \begin{pmatrix} w_-(x_1^{(N-1)} + \delta) \\ w_+(x_1^{(1)} - \delta) \end{pmatrix}. \quad (52)$$

However, for a guided mode we must have exponentially decaying scattered fields only, in both the substrate and the superstrate. That means that

$$w_+(x_1^{(1)} - \delta) = w_-(x_1^{(N-1)} + \delta) = 0. \quad (53)$$

Applying this to (52) leads to

$$\left(\mathbf{S}^{(1,N)}\right)^{-1} \begin{pmatrix} w_+(x_1^{(N-1)}) \\ w_-(x_1^{(1)}) \end{pmatrix} = \begin{pmatrix} 0 \\ 0 \end{pmatrix}. \quad (54)$$

These equations in $w_+(x_1^{(N-1)})$ and $w_-(x_1^{(1)})$ can only have a nontrivial solution if the determinant of $(\mathbf{S})^{-1}$, or the inverse of the determinant of $\mathbf{S}$, vanishes. Hence, we find the condition

$$\mathrm{Det}\left[\left(\mathbf{S}^{(1,N)}\right)^{-1}\right] = -\frac{q_{11}^{(1,N)}}{q_{22}^{(1,N)}} = 0. \quad (55)$$

It should be realized that the coefficients q are a function of the complex longitudinal propagation constant k_3, as can be seen from (41)–(44), (20), and (17). Since $q_{22}^{(1,N)}$ is a bounded function of k_3, the so-called dispersion relation reduces to

$$q_{11}^{(1,N)}(k_3) = 0. \quad (56)$$

From definition (47) it follows that

$$\mathbf{Q}^{(i,N)} = \mathbf{Q}^{(i)}\mathbf{Q}^{(i+1,N)}. \quad (1 \le i < N) \quad (57)$$

So the coefficient $q_{11}^{(1,N)}$ can be determined recursively through

$$q_{11}^{(i,N)} = q_{11}^{(i)} q_{11}^{(i+1,N)} + q_{12}^{(i)} q_{21}^{(i+1,N)}, \quad (58)$$

$$q_{21}^{(i,N)} = q_{21}^{(i)} q_{11}^{(i+1,N)} + q_{22}^{(i)} q_{21}^{(i+1,N)} \quad (59)$$

with $q_{ij}^{(i)}$ given by (41)-(44). The initialization is

$$\mathbf{Q}^{(N,N)} = \mathbf{I}. \quad (60)$$

Equations (58) and (59) are equivalent to the Redheffer star product for "multiplication" of scattering matrices [11]. They form a numerically stable method for determining $q_{11}^{(1,N)}(k_3)$ [12].

Only for a finite and discrete set of values of k_3 can the dispersion relation be satisfied. Those values are precisely the desired propagation constants of the guided modes of the planar waveguide. A standard root-finding routine (using Muller's method) is employed to find these zeroes of $q_{11}^{(1,N)}$ in the complex k_3 plane. Several limits for the TE roots can be estimated [13]. These can be used to limit the area of the plane in which the zeroes are sought. Further implementation details are given in [10].

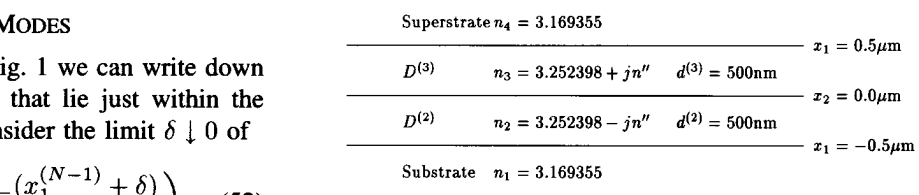

Fig. 3. Geometry of an asymmetric four-layer dielectric waveguide proposed by Nolting. The wavelength in vacuum $\lambda_0 = 1.55$ μm. n'' denotes the imaginary part of the index of refraction. This waveguide is studied in the very high gain and losses regime, i.e., for n'' relatively high.

A. Regaining the Field Distributions

We assume that $w_+(x_1^{(N-1)})$ is known up to some factor. For a guided mode $w_+(x_1^{(n-1)})$ and $w_-(x_1^{(n-1)})$ can then be expressed in this quantity with the help of (49) and (50)

$$w_+(x_1^{(n-1)}) = q_{11}^{(n,N)} w_+(x_1^{(N-1)}), \quad (61)$$

$$w_-(x_1^{(n-1)}) = q_{21}^{(n,N)} w_+(x_1^{(N-1)}). \quad (62)$$

So, for a point $x_1 \in D^{(n)}$ this leads to

$$\begin{pmatrix} w_+(x_1) \\ w_-(x_1) \end{pmatrix} = \begin{pmatrix} \exp[+\lambda_1^{(n)}(x_1 - x_1^{(n-1)})]\, q_{11}^{(n,N)} w_+(x_1^{(N-1)}) \\ \exp[-\lambda_1^{(n)}(x_1 - x_1^{(n-1)})]\, q_{21}^{(n,N)} w_+(x_1^{(N-1)}) \end{pmatrix}. \quad (63)$$

Using that $\mathbf{f}^{(n)}(x_1) = \mathbf{C}^{(n)}\mathbf{w}^{(n)}(x_1)$ eventually yields the desired expression for the electric and magnetic fields as a function of x_1, viz.

$$\tilde{E}_2^{(n)}(x_1) = (-j\omega\mu_0)^{1/2}\left(w_+^{(n)}(x_1) - w_-^{(n)}(x_1)\right), \quad (64)$$

$$\tilde{H}_3^{(n)}(x_1) = \left(\frac{jk_3k_3}{\omega\mu_0} - \omega\epsilon^{(n)}\right)^{1/2}\left(w_+^{(n)}(x_1) + w_-^{(n)}(x_1)\right) \quad (65)$$

$$\tilde{H}_1^{(n)}(x_1) = \frac{-k_3}{\omega\mu_0}\tilde{E}_2^{(n)}(x_1). \quad (66)$$

The expression for the third non-zero field component $\tilde{H}_1^{(n)}$ was obtained by using Eq. (13). The intensity I at a point $x_1 \in D^{(n)}$ is related with the Poynting vector as

$$I = \langle S_3 \rangle_T = \frac{1}{2}\mathrm{Re}\{\tilde{E}_2\tilde{H}_1^*\}. \quad (67)$$

Here, the symbol $\langle S_3 \rangle_T$ denotes the time-averaged longitudinal component of the Poynting vector.

To summarize, the roots of (56) represent the value of k_3 (and hence, the mode-index K) for a particular guided mode. Knowledge of k_3 allows computation of the coefficients q_{ij} of the scattering matrix. With the help of (64)–(66) the x_1-dependence of the fields can then be determined. That means that all elements of the desired guided mode solution of the form of (6) are now complete.

VII. Results

The first configuration that we study was suggested as a difficult modeling benchmark by H. P. Nolting in connection with the COST 240 project [14]. It is depicted in Fig. 3. This InGaAsP–InP waveguide consists of two embedded layers with identical real parts, but opposite imaginary parts of the index of refraction. It was found that this structure allows two

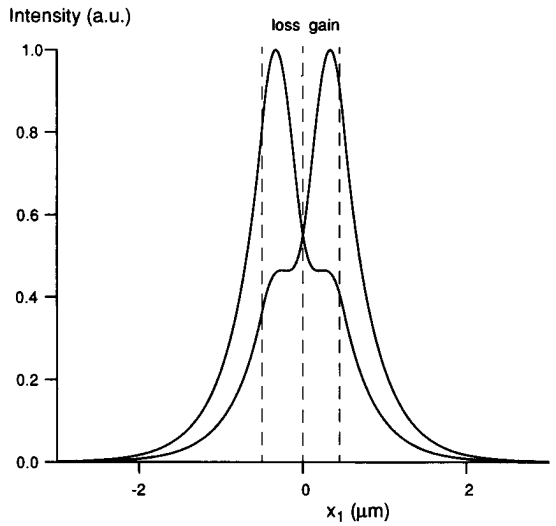

Fig. 4. Intensity profiles for the waveguide of Fig. 3 with $n'' = 0.07$. The three dashed lines indicate the boundaries between the layers. The two TE modes (at $\lambda_0 = 1.55$ μm) have equal real and opposite imaginary parts for their respective propagation constants.

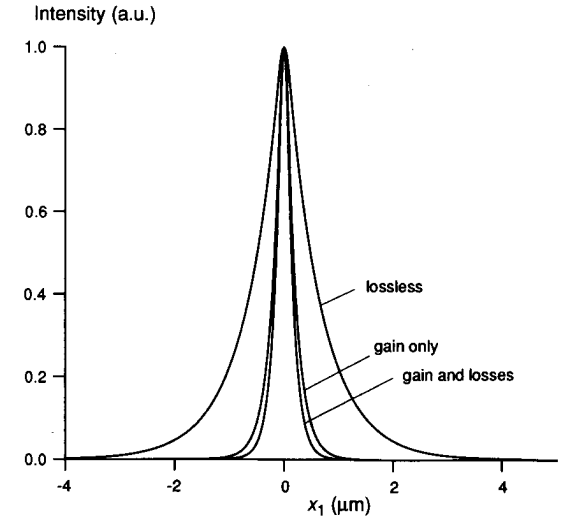

Fig. 5. Intensity profile for the TE_0 mode of a three-layer waveguide. If the central layer is active, the wave is much more confined than for the passive (i.e., lossless) case. If losses are included in the substrate and superstrate, the confinement gets even stronger.

TE modes at $\lambda_0 = 1.55$ μm. If $n'' < 0.064465$, then the imaginary part of the two-mode indexes is zero. For n'' larger than this value, the real parts of the two indexes coincide, whereas the imaginary parts are opposite. For the latter case, the intensity profiles for the two TE modes are plotted in Fig. 4 with $n'' = 0.07$. One mode, with gain, is predominantly located in the active layer. The other one, with loss, is the mirror image of the first with respect to the plane $x_1 = 0$. An identical behavior, but now around $n'' = 0.069229$, was found for the TM modes. Notice that values of n'' in this range correspond with extremely high gain and losses. Nevertheless, the scattering matrix method allows us to deal with this structure. Our results agree with Nolting's. This example demonstrates the usefulness of our approach.

Next, we study a symmetrical three-layer configuration with $n_1 = n_3 = 3.55$ and $n_2 = 3.60$. The thickness of layer $D^{(2)}$ is 200 nm, and $\lambda_0 = 1.3$ μm. In Fig. 5, the intensity profile along the x_1-direction is plotted for the TE_0 mode. If a positive imaginary part is added to n_2 (i.e., layer $D^{(2)}$ becomes active), e.g., $n_2 = 3.60 + j\ 0.50$, the wave gets more confined to the central layer. This effect is enhanced if the two outer layers become lossy with $n_1 = n_3 = 3.55 - j\ 0.15$. In this example we have a relatively small refractive index step and a very large gain, to show the effects of gain and losses on confinement. It should be remarked that the increased confinement practically does not occur in other more realistic configurations, e.g., when $n_1 = n_3 = 3.20$ and $n_2 = 3.60$ (core thickness again 200 nm, $\lambda_0 = 1.3$ μm). The confinement factor for the TE_0 mode is now 56.8%. Introducing gain and losses by taking $n_1 = n_3 = 3.20 - j\ 0.01$ and $n_2 = 3.60 + j\ 0.10$, merely changes the confinement to 57.1%.

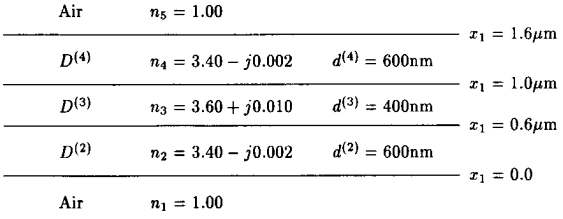

Fig. 6. Geometry of a five-layer dielectric waveguide with both gain and losses. $D^{(3)}$ is the active layer. The wavelength in vacuum $\lambda_0 = 1.3$ μm.

TABLE I
GAIN AND LOSS MODES FOR TE AND TM FIELDS IN A FIVE-LAYER WAVEGUIDE

mode	gain (dB)/100μm	mode index $K = k_3/k_0$
TE_0	29.82	$3.50344333295 + j7.10300097868E-03$
TE_1	−0.96	$3.33728685820 - j2.29491104011E-04$
TE_2	−2.23	$3.25168520698 - j5.30514779910E-04$
TE_3	5.62	$3.10425142141 + j1.33798633975E-03$
TE_4	−0.73	$2.87863677988 - j1.73729890360E-04$
TE_5	6.50	$2.62813932045 + j1.54864433114E-03$
TE_6	2.97	$2.24395136260 + j7.08377958008E-04$
TE_7	5.68	$1.76819096041 + j1.35321718386E-03$
TE_8	10.32	$1.07426202652 + j2.45789147357E-03$
TM_0	27.47	$3.49668379589 + j6.54398171098E-03$
TM_1	0.14	$3.33069711910 + j3.51864222567E-05$
TM_2	−0.73	$3.22433799874 - j1.74482612621E-04$

The next example is the five-layer dielectric structure that is depicted in Fig. 6. All TE modes, plus the first three TM modes are given in Table I. Listed are the mode indexes which are defined as $K = k_3/k_0$, with k_0 the free-space wave number. While the first TE mode is a gain mode, the next two TE modes are loss modes. The higher order modes show a seemingly random alternation of loss and gain modes. For the TM field all higher order modes (not tabulated) are gain modes for this particular case. The intensity distribution along the lateral x_1-direction, as depicted in Fig. 7 for two TE modes, gives some indication. Since the TE_0 mode is seen to be mainly confined to the active layer, it comes as no surprise that this a gain mode. Likewise, the intensity for the TE_1 mode is relatively low in the central layer and this is, indeed, a loss mode.

We can also study what happens with the TE_0 mode for this configuration when the imaginary part of n_3 is gradually decreased. This is plotted in Fig. 8, which shows the loci of the mode index $K = k_3/k_0$ with Im $\{n_3\}$ as a parameter. As expected, the imaginary part of the index is lowered, which means a lesser gain per unit length, for a decrease in the Im $\{n_3\}$. For n_3 purely real the TE_0 mode is already a loss mode

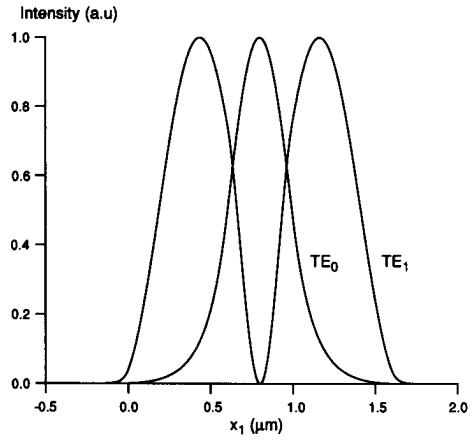

Fig. 7. Intensity profiles for the TE_0 and TM_1 modes of the five-layer waveguide of Fig. 6.

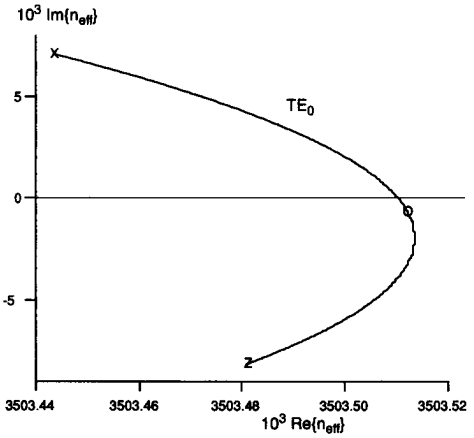

Fig. 8. Effective index loci for theTE_0 mode of a five-layer waveguide for varying imaginary part of the refractive index of the central layer $D^{(3)}$. X: $\mathrm{Im}\{n^{(3)}\} = 0.01$, O:$\mathrm{Im}\{n^{(3)}\} = 0.00$, Z: $\mathrm{Im}\{n^{(3)}\} = -0.01$.

with a negative imaginary part. For Im $\{n_3\} < 0$, the real part of the mode index gets smaller, whereas the imaginary part increases.

In Fig. 9, the root loci are shown for a decreasing thickness $d^{(3)}$ of the gain layer. For all modes the real part of the index decreases with decreasing thickness. The TE_0 mode, which is originally a gain mode, shows less gain with decreasing layer thickness and eventually becomes a loss mode.

In general, there is a substantial gain difference between TE and TM modes, even though the permittivity ϵ that we consider is a scalar. In the waveguide under consideration, the TM_0 gain per length is almost 10% less than that of the TE_0 mode, as can be gathered from Table I. For planar dielectric waveguides the mode with the lowest cutoff frequency is always TE_0. The confinement for this mode and hence, the gain in case of active media is therefore greater than for the TM_0 mode. We return to the connection between gain and confinement in the next example.

As a model of a realistic semiconductor amplifier we examine the configuration of Fig. 10. It consists of a InP substrate, and an InGaAsP active layer, which is sandwiched between a n-doped and a p-doped layer of InP. On top a thin gold contact layer is deposited. The imaginary parts of the index of refraction of the doped InP layers correspond with

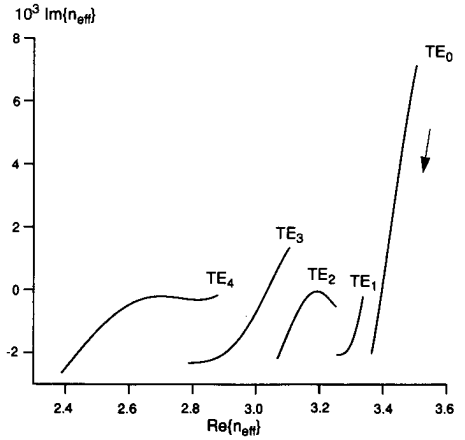

Fig. 9. Effective index loci for decreasing thickness $d^{(3)}$ of the active layer of a five-layer waveguide. All modes move in the direction of decreasing $\mathrm{Re}\{n_{\mathrm{eff}}\}$ with decreasing thickness (see arrow). Eventually all modes are lossy. The thickness is varied from 0.4 μm to zero.

Air	$n_6 = 1.00$		$x_1 = 4.19\mu m$
Au	$n_5 = 0.18 - j10.2$	$d^{(5)} = 40nm$	$x_1 = 4.15\mu m$
p-InP	$n_4 = 3.16 - j0.0001$	$d^{(4)} = 1.0\mu m$	
			$x_1 = 3.15\mu m$
InGaAsP	$n_3 = 3.60 + j0.002$	$d^{(3)} = 150nm$	
			$x_1 = 3.00\mu m$
n-InP	$n_2 = 3.16 - j0.0001$	$d^{(2)} = 3.0\mu m$	
			$x_1 = 0.0$
InP	$n_1 = 3.16$		

Fig. 10. Geometry of a planar optical amplifier with both gain and losses. The wavelength in vacuum $\lambda_0 = 1.3$ μm. The gain of this device is very sensitive to the state of polarization. N. B. vertical distances are not true to scale.

doping levels of the order of $10^{18}/cm^3$ [15]. It is found that at $\lambda_0 = 1.3$ μm only one guided TE and one guided TM mode can be sustained. It was found that the sensitivity of the gain to the state of polarization is very great. For an active layer thickness of 150 nm, the TE gain is almost twice as great as that for the TM, namely 3.84 dB/100 μm against 2.29. Contrary to what is sometimes thought, the confinement (i.e., the percentage of the intensity of the mode in the active layer) is quit similar for the two modes (45% for TE against 41% for TM). The role of the confinement factors and their relation with the modal gain is elucidated in [6]. The difference in gain is due to the difference in the imaginary part of the effective index of the two modes. It was found that $n_{\mathrm{eff}} = 3.2808 + j\ 9.139 \times 10^{-4}$ and $n_{\mathrm{eff}} = 3.2480 + j\ 5.463 \times 10^{-4}$ for TE and TM, respectively.

Due to the good confinement, the presence of the thin Au contact layer makes very little difference to the mode indexes. So, in most practical situations one does not have to take this layer into account.

Finally, we studied the frequency dependent permittivity ϵ by taking six closely spaced Lorentz lines [see (5)] around $\lambda_0 = 1.3$ μm. Five lines were emission lines and one described absorption. Constructing the gain profile this way ensures that the complex permittivity $\epsilon(\omega)$ satisfies the Kramers-Kronig causality relations. The resulting $\mathrm{Im}\{\epsilon\}$ profile of Fig. 11 is similar to measured gain profiles [16, ch. 3]. As can be seen from Fig. 12 the TE_0 gain for this profile can be up to two times greater than that for the TM_0 mode. Also, the width of

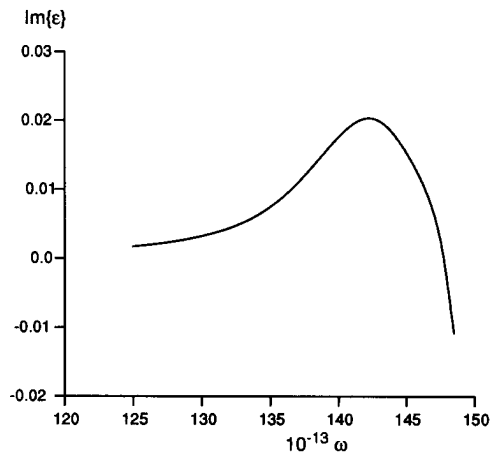

Fig. 11. The imaginary part of the permittivity ϵ versus ω for the InGaAsP gain layer $D^{(3)}$. This profile is the sum of five Lorentzian emission and one absorption line. The peak at $\lambda_0 = 1.325$ μm corresponds with a bulk gain exponent of 268 cm^{-1}.

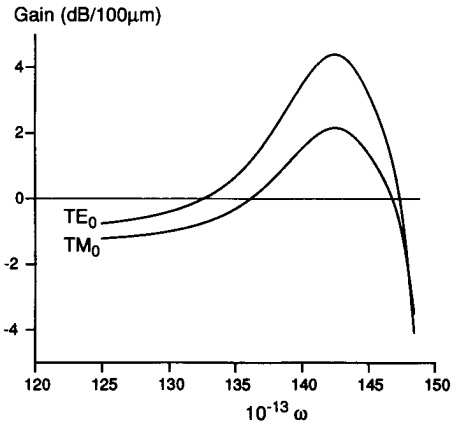

Fig. 12. Gain in dB per 100 μm for the TE_0 and TM_0 modes as a function of ω for a semiconductor laser amplifier. At the resonance frequency (corresponding with $\lambda_0 = 1.32$ μm) theTE_0 gain is 103% larger than the TM_0 gain. Off resonance, both modes become lossy, but the TM_0 mode does so first.

the TE profile is substantially larger. Off resonance both modes eventually become lossy, but the TM_0 mode does so first.

The difference in gain between TE and TM modi for laser amplifiers with thin ($\sim$100 nm) active layers is usually accredited to a difference in confinement factors. The present authors do not entirely agree with that view. In the first place, we have shown that even with similar confinement factors there may still be a substantial difference in gain. In the second place, contrary to conventional wisdom, the relation between modal gain and confinement factors for TE differs from that for TM [6].

VIII. Conclusion and Discussion

We have used a scattering matrix approach to study the waveguiding properties of planar configurations with strong losses and gain. Contrary to the usually applied transfer matrix method, the model that we use is numerically stable. Even configurations with very strong losses and gain can easily be dealt with.

It was seen that increasing the gain in the active layer causes the fields to be more confined.

For realistic semiconductor laser amplifiers with losses in the embedding around the active layers, the gain is found to be very sensitive to the state of polarization. The TE gain (in dB/100 μm) can be 100% greater than that for the TM mode. This is in agreement with measurements.

From this study we conclude that isotropic planar amplifiers inherently posses a significant gain sensitivity to the state of polarization. That means that in order to achieve the desired polarization independence one must resort to an anisotropic active layer, and/or to two-dimensional devices, such as ridge waveguides.

Acknowledgment

One of the authors, T. D. Visser, would like to thank Mathé van Stralen for letting him use his software.

References

[1] L. F. Tiemeijer, P. J. A. Thijs, T. van Dongen, R. W. M. Slootweg, J. M. M. van der Heijden, J. J. M. Binsma, and M. P. C. M. Krijn, "Polarization insensitive multiple quantum well laser amplifiers for the 1300 nm window," *Appl. Phys. Lett.*, vol. 62, pp. 826–828, 1993.
[2] K. S. Chiang, "Review of numerical and approximate methods for the modal analysis of general optical dielectric waveguides," *Opt. Quantum Electron.*, vol. 26, pp. S113–S134, 1994.
[3] D. Yevick, "A guide to electric field propagation techniques for guided-wave optics," *Opt. Quantum Electron.*, vol. 26, pp. S185–S198, 1994.
[4] S. Shimada and H. Ishio, Eds., *Optical Amplifiers and Their Applications*. New York: Wiley, 1994.
[5] T. Saitoh and T. Mukai, "1.5 μm GaInAsP traveling-wave semiconductor laser amplifier," *IEEE J. Quantum Electron.*, vol. 23, pp. 1010–1020, 1987.
[6] T. D. Visser, B. Demeulenaere, J. Haes, D. Lenstra, R. Baets, H. Blok, "Two identities for the effective index of guided modes in slab waveguides," submitted for publication to *J. Lightwave Technol.*
[7] R. J. Hawkins and J. S. Kalman, "Lasing in tilted-waveguide semiconductor laser amplifiers," *Opt. Quantum Electron.*, vol. 26, pp. S207–S219, 1994.
[8] R. H. Pantell and H. E. Puthoff, *Fundamentals of Quantum Electronics*. New York: Wiley, 1969.
[9] C. Vassallo, *Optical Waveguide Concepts*. Amsterdam: Elsevier, 1991.
[10] M. J. N. van Stralen, Internal Rep. Et/EM 1992-03, Delft Univ. Technol., (available on request from H. Blok).
[11] R. Redheffer, "On the reation of transmission-line theory to scattering and transfer," *J. Math. Phys.*, vol. 41, pp. 1–41, 1962.
[12] D. Ko and J. Sambles, "Scattering matrix method for propagation of radiation in stratified media: Attenuated total reflection studies of liquid crystals," *J. Opt. Soc. Am. A*, vol. 5, pp. 1863–1866, 1988.
[13] H. M. de Ruiter, "Limits on the propagation constants of planar optical waveguides modes," *Appl. Opt.*, vol. 20, pp. 731–732, 1981.
[14] H. P. Nolting, private communication
[15] R. G. Hunsperger, *Integrated Optics: Theory and Technology*. Berlin: Springer-Verlag, 1984.
[16] G. P. Agrawal and N. K. Dutta, *Long-Wavelength Semiconductor Lasers*. New York: Van Nostrand Reinhold, 1986.

T. D. Visser, photograph and biography not available at the time of publication.

H. Blok (M'87), photograph and biography not available at the time of publication.

D. Lenstra, photograph and biography not available at the time of publication.